

DISPEL: Domain Generalization via Domain-Specific Liberating

Chia-Yuan Chang
Texas A&M University
cychang@tamu.edu

Yu-Neng Chuang
Rice University
ynchuang@rice.edu

Guanchu Wang
Rice University
gw22@rice.edu

Mengnan Du
New Jersey Institute of Technology
mengnan.du@njit.edu

Na Zou
Texas A&M University
nzoul@tamu.edu

Abstract

Domain generalization aims to learn a generalization model that can perform well on unseen test domains by only training on limited source domains. However, existing domain generalization approaches often bring in prediction-irrelevant noise or require the collection of domain labels. To address these challenges, we consider the domain generalization problem from a different perspective by categorizing underlying feature groups into domain-shared and domain-specific features. Nevertheless, the domain-specific features are difficult to be identified and distinguished from the input data. In this work, we propose *Domain-Specific Liberating (DISPEL)*, a post-processing fine-grained masking approach that can filter out undefined and indistinguishable domain-specific features in the embedding space. Specifically, DISPEL utilizes a mask generator that produces a unique mask for each input data to filter domain-specific features. The DISPEL framework is highly flexible to be applied to any fine-tuned models. We derive a generalization error bound to guarantee the generalization performance by optimizing a designed objective loss. The experimental results on five benchmarks demonstrate DISPEL outperforms existing methods and can further generalize various algorithms.

1. Introduction

Deep neural network (DNN) models have achieved impressive results in various fields, including object recognition [47, 36, 13, 3, 10], semantic segmentation [34, 11, 49, 45, 53], and object detection [12, 21, 37, 5, 8, 48]. However, the distribution of test data in the real-world applications may be statistically different from training data, causing DNN models to severely suffer performance drops. In this case, domain generalization research aims to address the challenges of distribution difference, known as the do-

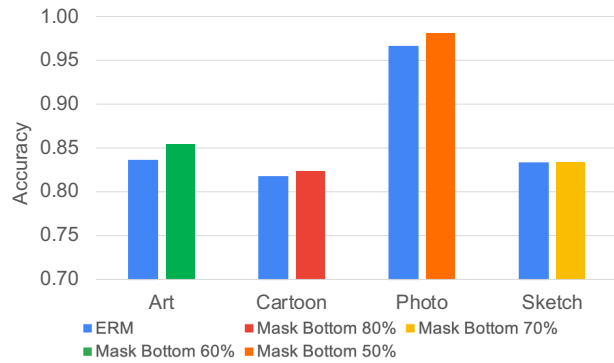


Figure 1: Efficacy of Global Masking (see Sec. 2.2) on each unseen domain of the PACS dataset. The Mask Bottom p% describes the percentage of masked embedding dimensions. We present the most effective p% for each unseen domain.

main shifting problem. Domain generalization is essential for real-world applications where collecting representative training data may be difficult or costly. Therefore, it is crucial to have models with good generalization properties trained on limited domain training data.

Existing algorithms for domain generalization can be categorized into two branches: data manipulation and representation learning. The first branch, data manipulation [38, 39, 43, 42, 33, 50, 51, 31], focuses on reducing overfitting issues by increasing the diversity and quantity of available training data through data augmentation methods or generative models. Two well-known studies in this branch are Mixup [52, 46] and Randomization [29]. The second branch, representation learning [22, 19, 23, 25, 17, 27, 26, 9, 30, 7], aims to learn an encoder that generates invariant embeddings among different domains. This branch includes popular algorithms such as CORAL [35], IRM [1], and DRO [32]. Beyond algorithms design, model selection during the training stage can also influence generalization performance. A recent research [18] proposes

two model selection settings in which the selected models can be trained to achieve good generalization results. However, there are several limitations among existing approaches. First, data manipulation methods require highly engineered efforts and can introduce too much prediction-irrelevant knowledge label noise, which will degrade prediction performance. Second, the penalty regularizations of representation learning often require domain labels or information to train domain-invariant encoder; and the existing model selection settings also need the use of domain labels to obtain desirable validation subsets. Nonetheless, obtaining these domain labels can be a significant expense or may not be feasible in real-world applications.

To develop a novel solution branch without the limitations above, we consider the domain generalization problem from a different perspective by categorizing underlying feature groups, i.e., *domain-shared and domain-specific features*. The domain-shared features generally exist in all domains, and the domain-specific features only exist in certain domains. The prediction models typically experience a drop in performance when tested on unseen domains that are excluded in training data. This is because the prediction models are trained on both domain-shared and domain-specific features, which leads to ineffective prediction outcomes on unseen domain data. Intuitively, we can make a prediction model independent of domain-specific features by eliminating them during inference. However, there are two difficulties in using this intuition. First, domain-specific features are usually hard to be identified or predefined because those features are represented in different formats. For instance, one domain-specific feature could be the color of objects in a source domain. This means that an object’s color is highly correlated with its ground truth. Nevertheless, when the domain-specific features are the interweaved relationship between an object’s color and stripe, it becomes difficult to recognize the correlation between each domain-specific feature and the ground truths. Second, domain-specific features are typically difficult to be distinguished directly from the original image. Taking an “Art style” car image as an example. It is impalpable what is the “Art style” car image, which only includes domain-specific features, and what is the car image without any “style,” which only contains domain-shared features.

To address the two difficulties, we perform a post-processing method, a global mask, to filter out domain-specific features in the latent space. We verify its efficacy by designing a naive global mask to filter out the domain-specific features. The global mask is identified by ranking the Permutation Importance [16] of each embedding dimension. The results in Fig. 1 show that utilizing the global mask can improve the generalization performance of a fine-tuned¹ model on different unseen domains. However, it is a

sub-optimal solution since the global mask does not account for the discrepancy among training instances. As illustrated in Fig. 1, the effectiveness of masked dimensions varies for different compositions of training domains.

To account for instance discrepancies among various training domains without relying on domain labels, we propose DomaIn-SPEcific Liberating (DISPEL), a post-processing fine-grained masking approach that extracts out domain-specific features in the embedding space. Our proposed framework is illustrated in Fig. 2. **The key idea of DISPEL is to learn a mask generator that automatically generates a distinct mask for each input data, which is to filter domain-specific features from the embedding space.** The effectiveness of the proposed DISPEL is theoretically and empirically demonstrated to improve generalization performance, without utilizing domain labels. The experimental results on five benchmark datasets indicate that the proposed DISPEL achieves state-of-the-art performance, even without leveraging domain labels and any data augmentation method. This performance exceeds that of algorithms that require domain labels for training.

Our main contributions are as follows:

- We propose DISPEL to generalize a frozen model by masking out hard-to-identify domain-specific features in the embedding space without adopting domain labels.
- Theoretical analysis guarantees that DISPEL improves the generalization performance of frozen prediction models by minimizing the generalization error bound.
- Experimental results on various benchmarks demonstrate the effectiveness of DISPEL and it can also further improve the existing domain generalization algorithms.

2. A Naive Method with Global Masking

In this section, we will go over the notations used in this paper and demonstrate the efficacy and limitation of a naive global masking strategy.

2.1. The Problem of Domain Generalization

A domain is a collection of data drawn from a distribution. Given a training domain set \mathcal{X} with a label set \mathcal{Y} , the goal of domain generalization is to find a perfect generalized model $f : \mathcal{X} \rightarrow \mathcal{Y}$ with parameter $\theta \in \Theta$ that can perform well on both training domains and unseen test domains. Note that unseen test domains are not included in training domains. Let $\mathcal{X} := \{\mathcal{D}_i\}_{i=1}^I$ be a set of training domains and \mathcal{D}_i be a distribution over input space \mathcal{X} , where I denotes the total number of training domains. We denote each training domain as $\mathcal{D}_i = \{\mathbf{x}_j^i\}_{j=1}^{\mathcal{J}}$ and define a set of

¹ther trained on a specific task using a training set, where the pre-trained model is pre-trained on a large-scale dataset such as ImageNet.

¹A fine-tuned model refers to the pre-trained model that has been fur-

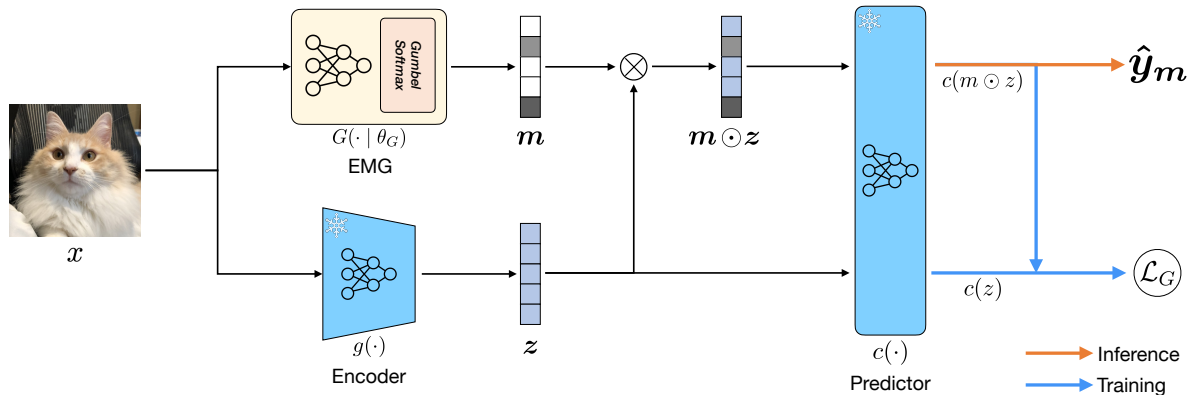


Figure 2: An overview of the proposed framework DISPEL, where EMG refers to Embedding Mask Generator (see Sec. 3.2), and \mathcal{L}_G denotes the objective loss (see Eq. 3). The framework DISPEL first splits a given frozen fine-tuned model into an encoder $g(\cdot)$ and a predictor $c(\cdot)$, and then updates EMG by minimizing cross entropy loss between $c(m \odot z)$ and $c(z)$.

unseen domain samples $\mathcal{T} := \{\mathbf{x}_k^T\}_{k=1}^K$, where \mathcal{J} denotes the total number of training domain samples and K represents the total number of unseen domain samples.

2.2. Globally Masking Domain-Specific Features

The performance of prediction models is typically degraded while testing on unseen domains due to accounting for domain-specific features. We experimentally show that masking out the domain-specific features in embedding space during inference can improve the generalization ability of prediction models. Specifically, given a prediction model, we split it into an encoder for mapping input data to embedding space, and a predictor for predicting. Then we leverage a feature explainer for calculating important scores for each embedding dimension, assuming that the less accumulated important scores among training data indicate the more domain-specific dimensions. Following this idea, a global mask can be found by identifying a certain number of domain-specific dimensions. Then we can leverage it to block out the domain-specific embedding dimensions to make the predictor focus on domain-shared features. In our following experiment, the global masks are obtained by calculating permutation importance [16]. The results on the PACS dataset shown in Fig. 1, demonstrating that prediction accuracy on unseen domains of a fine-tuned ERM model can be improved by a global mask blocking out a certain percent of dimensions.

Despite of the efficacy of the global masking method, it is a sub-optimal solution because a global mask cannot consider the discrepancy among instances of different domains for each sample. As shown in Fig. 1, the effectiveness of masked embedding dimensions varies among different compositions of training domains. In other words, the improvements raised by a single global mask will vary among different unseen domains.

3. Domain-Specific Liberating (DISPEL)

To address the limitation of the global masking method as is introduced in Sec. 2.2, we aim to achieve domain generalization by considering a fine-grained masking method. To this end, in this section, we formally propose the DomaIn-SpEcific Liberating (DISPEL) framework that prevents a prediction model from focusing on domain-specific features projected on the dimensions of each embedding.

3.1. Overall DISPEL Framework

The prediction models being fine-tuned with ERM may have limited generalization performance on an unseen test domain. To address this, we introduce DISPEL, a post-processing domain generalization framework that enhances the fine-tuned model’s generalization performance without modifying its parameters. Specifically, DISPEL improves its generalization by accounting for instance discrepancies among various training domains without using domain labels. We propose a fine-grained masking component named Embedding Mask Generator (EMG) that can generate instance-specific masks for blocking the domain-specific features in the embedding space (see Fig. 2). The framework of DISPEL is given as follows. Generally, we freeze the prediction model and split it into an encoder $g(\cdot) : \mathcal{X} \rightarrow \mathcal{Z}$ and a predictor $c(\cdot) : \mathcal{Z} \rightarrow \mathcal{Y}$, where \mathcal{Z} is the embedding space mapped by $g(\cdot)$. Given an input instance $\mathbf{x} \in \mathcal{X}$, EGM can generate a mask \mathbf{m} for embedding \mathbf{z} of the input data to filter domain-specific features, where the embedding is encoded by the encoder $g(\mathbf{x}) = \mathbf{z}$. Finally, the frozen model can achieve domain generalization on the unseen test domain via the mask generated by EMG. We will introduce the implementation details in Sec. 4.1. In the following, we will introduce the details and training process of the proposed EMG component.

3.2. Embedding Mask Generator (EMG)

Considering the inherent problem among training data from different domains, the Embedding Mask Generator (EMG) $G : \mathcal{X} \rightarrow \mathbb{R}^d$ aims to generate an instance-specific mask to mask out domain-specific features corresponding to the input data in embedding space. Specifically, for a data instance \mathbf{x} , a domain-specific embedding mask is generated to satisfy d -dimensional Binomial distribution $\mathcal{B}(1 - p_1, \dots, 1 - p_d)$, where $[p_1, \dots, p_d] = G(\mathbf{x} \mid \theta_G)$. To enable the updating of the base model of the EMG $G(\cdot \mid \theta_G)$ through backward propagation, a temperature-dependent Gumbel Softmax operation is adopted. Formally, the embedding mask is generated as follows:

$$\mathbf{m}_j^i = \frac{\exp\{(\log(\mathbf{1} - \mathbf{p}) + \mathbf{h})/\tau\}}{\exp\{(\log(\mathbf{1} - \mathbf{p}) + \mathbf{h})/\tau\} + \exp\{(\log(\mathbf{p}) + \mathbf{h}')/\tau\}} \quad (1)$$

where $\log(\cdot)$ and $\exp(\cdot)$ denote the element-wise operation of a vector; τ is a temperature hyper-parameter for controlling the degree of discreteness of the generated distribution; and $\mathbf{h} = [h_1, \dots, h_d]$ and $\mathbf{h}' = [h'_1, \dots, h'_d]$ are randomly sampled from d -dimensional standard Gumbel distribution $\text{Gumbel}(\mathbf{0}, \mathbf{1})$:

$$\text{Gumbel}(\mathbf{0}, \mathbf{1}) = -\log(-\log u), u \sim \text{Uniform}(0, 1). \quad (2)$$

The τ in the Gumbel Softmax operation is an implicit regularization that can be used to avoid the trivial solution of EMG outputting all one mask.

3.3. The Training of EMG Module

The goal of DISPEL is to improve the generalization of a frozen prediction model by preserving domain-shared features while filtering out domain-specific features via $\mathbf{m}_j^i \odot \mathbf{z}_j^i$. To achieve the goal, the output of frozen predictor with a masked embedding $c(\mathbf{m}_j^i \odot \mathbf{z}_j^i) = \hat{\mathbf{y}}_m$ should be close to the one without being masked $c(\mathbf{z}_j^i) = \hat{\mathbf{y}}$ for all $\mathbf{z}_j^i \in \mathcal{Z}$ and $1 \leq j \leq \mathcal{J}$. Following this intuition, EMG can be updated by minimizing the cross entropy loss L_{CE} between $c(\mathbf{m}_j^i \odot \mathbf{z}_j^i)$ and $c(\mathbf{z}_j^i)$ as follows:

$$\begin{aligned} \mathcal{L}_G &= \min_{\theta_G} \sum_{i=1}^I \sum_{j=1}^{\mathcal{J}} L_{CE}(c(\mathbf{m}_j^i \odot \mathbf{z}_j^i), c(\mathbf{z}_j^i)) \\ &= \min_{\theta_G} \sum_{i=1}^I \sum_{j=1}^{\mathcal{J}} L_{CE}(\hat{\mathbf{y}}_m, \hat{\mathbf{y}}). \end{aligned} \quad (3)$$

The trained EMG $G(\cdot \mid \theta_G)$ is a domain-specific feature mask generator across multiple domains, which does not require domain labels for training.

3.4. Generalization Bound of DISPEL

The objective function of EMG module in Eq. 3 aims to mitigate the performance drop on unseen test domains,

which is caused by domain-specific features. The generalization error is thereby amply due to the impact of domain-specific features. In this section, we provide Theorem 1 to show that the generalization error can be effectively bounded by DISPEL, referring to a better DG capability across the unseen domains.

Theorem 1 (Generalization Error Bound). *Let $\tilde{\mathbf{x}}_k^T$ be a masked instance of \mathbf{x}_k^T on an unseen domain T . Given an instance embedding \mathbf{z}_k^T satisfies the composition of domain-specific \mathbf{z}_k^{T-sp} and domain-sharing \mathbf{z}_k^{T-sh} , where $\hat{f}(\mathbf{x}_k^T) = \hat{c}(\mathbf{z}_k^T)$ be the predicted outcomes. For arbitrary distance function $d(\cdot, \cdot)$ in metric space, the generalization error $\mathbf{GE} = \mathbf{E}_{\mathcal{X}}[d(f(\mathbf{x}_k^T), \hat{f}(\tilde{\mathbf{x}}_k^T))]$ of DISPEL framework can be bounded as:*

$$\mathbf{GE} \leq \mathbf{E}_{\mathcal{X}}[d(c(\mathbf{z}_k^{T-sh}), \hat{c}(\tilde{\mathbf{z}}_k^{T-sh}))] + \mathbf{E}_{\mathcal{X}}[d(c(\mathbf{z}_k^{T-sp}), \hat{c}(\tilde{\mathbf{z}}_k^{T-sp}))] \quad (4)$$

where $\tilde{\mathbf{z}}_k^T = \mathbf{z}_k^T \odot \mathbf{m}_k^T$ is composed of remained domain-specific embedding $\tilde{\mathbf{z}}_k^{T-sp}$ and preserved domain-sharing embedding $\tilde{\mathbf{z}}_k^{T-sh}$.

Theorem 1 shows that the upper bound of the GE depends on two terms, which are the predicted error of domain-shared features and of domain-specific features. The proof of Theorem 1 is provided in Appendix A. Based on Eq. 5, DISPEL contributes to minimizing the upper bound of GE as follows:

- The objective loss of EMG in Eq. 3 aligns with the goal of minimizing the first term of Theorem 1, as \mathbf{m}_k^T aims to preserve the domain-shared features on \mathbf{z}_k^{T-sh} for the prediction of multiple training domains.
- DISPEL framework minimizes the value of second terms in Eq. 5 by making $\tilde{\mathbf{z}}_k^{T-sp}$ approaches \mathbf{z}_k^{T-sp} with a generated mask.

3.5. Algorithm of EMG Training

The training outline of the EMG is given in Algorithm 1. The training aims to achieve the base model of EMG $G(\cdot \mid \theta_G)$ that can generate domain-specific feature masks for each input data. Specifically, EMG generates instance-specific embedding masks based on given training data (line 4), and then we let the frozen predictor $c(\cdot)$ predicts given masked embedding and original embedding (line 5-6). In each iteration, EMG is updated according to Eq. 3 (line 7) until it converges.

4. Experiments

In this section, we conduct experiments to evaluate the performance of DISPEL framework, aiming to answer the following three research questions: **RQ1:** How effective is the proposed DISPEL when compared to state-of-the-art

Algorithm 1 Embedding Mask Generator (EMG) Training1: **Input:**

Training dataset $\mathbf{x} \in \mathcal{X}$
 Frozen feature encoder $g(\mathbf{x}) = \mathbf{z}$
 Frozen predictor $c(\cdot)$
 Base model of EMG $G(\cdot | \theta_G)$

2: **Output:**

Instance-specific mask generator EMG $G(\cdot | \theta_G)$

3: **while** not convergence **do**

4: Generate the embedding mask \mathbf{m} by $G(\mathbf{x} | \theta_G)$ and Eq. 1

5: Predict by $c(\cdot)$ given masked embedding $\hat{\mathbf{y}}_{\mathbf{m}} = c(\mathbf{m} \odot \mathbf{z})$

6: Predict by $c(\cdot)$ given original embedding $\hat{\mathbf{y}} = c(\mathbf{z})$

7: Update $G(\cdot | \theta_G)$ by minimizing the objective loss Eq. 3

8: **end while**

baselines? **RQ2:** How does the fine-grained masking manner influence generalization performance? **RQ3:** Can DISPEL improve the generalization of other algorithms?

Table 1: Average unseen domain results (ResNet50).

	PACS	Office-Home	VLCS	TerraInc	DomainNet	Avg.
Group 1: algorithms requiring domain labels						
Mixup [46]	87.7 ± 0.5	71.2 ± 0.1	77.7 ± 0.4	48.9 ± 0.8	39.6 ± 0.1	65.1
MLDG [23]	84.8 ± 0.6	68.2 ± 0.1	77.1 ± 0.4	46.1 ± 0.8	41.8 ± 0.4	63.6
CORAL [35]	86.2 ± 0.2	70.1 ± 0.4	77.7 ± 0.5	46.4 ± 0.8	41.8 ± 0.2	64.4
MMD [25]	87.1 ± 0.2	70.4 ± 0.1	76.7 ± 0.9	49.3 ± 1.4	39.4 ± 0.8	64.6
DANN [17]	86.7 ± 1.1	69.5 ± 0.6	78.7 ± 0.3	48.4 ± 0.5	38.4 ± 0.0	64.3
C-DANN [27]	82.8 ± 1.5	65.6 ± 0.5	78.2 ± 0.4	47.6 ± 0.8	38.9 ± 0.1	62.6
DA-ERM [14]	84.1 ± 0.5	67.9 ± 0.4	78.0 ± 0.2	47.3 ± 0.5	43.6 ± 0.3	64.2
Group 2: algorithms without requiring domain labels						
ERM [40]	86.4 ± 0.1	69.9 ± 0.1	77.4 ± 0.3	47.2 ± 0.4	41.2 ± 0.2	64.5
IRM [1]	84.4 ± 1.1	66.6 ± 1.0	78.1 ± 0.0	47.9 ± 0.7	35.7 ± 1.9	62.5
DRO [32]	86.8 ± 0.4	70.2 ± 0.3	77.2 ± 0.6	47.0 ± 0.3	33.7 ± 0.2	63.0
RSC [19]	86.9 ± 0.2	69.4 ± 0.4	75.3 ± 0.5	45.7 ± 0.3	41.2 ± 1.0	63.7
MIRO [7]	85.4 ± 0.4	70.5 ± 0.4	79.0 ± 0.0	50.4 ± 1.1	44.3 ± 0.2	65.9
DISPEL	88.2 ± 0.1	73.3 ± 0.3	79.3 ± 0.1	50.4 ± 0.2	44.1 ± 0.0	67.1

4.1. Experimental Settings

Datasets. To compare the efficacy of our proposed framework with existing algorithms, we conduct our experiments on five real-world benchmark datasets: PACS [24] with 7 classes of images in 4 domains, Office-Home [41] with 65 classes of images in 4 domains, VLCS [15] with 5 classes of images in 4 domains, Terra Incognita [4] with 10 classes of images in 4 domains, and DomainNet [28] with 345 classes of images in 6 domains. DomainNet can be considered a larger-scale dataset with a more difficult multi-classification task than the other 4 benchmark datasets. More details about the datasets can be found in Appendix C.

Baselines. To fairly compare our proposed framework with existing algorithms, we follow the settings of DomainBed [18] and DeepDG [44], using the best result between DomainBed, DeepDG, and the original literature. We categorize the 12 baseline algorithms into two groups: **Group 1:** the algorithms requiring domain labels (Mixup [46], MLDG [23], CORAL [35], MMD [25],

DANN [27], C-DANN [27], and DA-ERM [14]); and **Group 2:** the algorithms without requiring domain labels (ERM [40], IRM [1], DRO [32], RSC [19], and MIRO [7]). More baselines details can be found in Appendix D.

Implementation Details. All the experimental results of the proposed DISPEL are implemented and performed based on the codebase of DeepDG [44]. Regarding the setting of model selection, we use traditional *training-domain validation set* for our implementation. Since larger ResNets are known to have better generalization ability, we mainly conduct experiments with ResNet50 models for all 5 benchmark datasets, and also show the results of DISPEL based on ResNet18 as a reference in Tab. 2. For all the experimental results of DISPEL, we employ ERM to fine-tune the pre-trained ResNet18 and ResNet50 as the fine-tuned model mentioned in Sec. 3.1. As for the EMG module in DISPEL, we employ a pre-trained ResNet50 as the base model and set the temperature hyper-parameter τ in Eq. 1 to 0.1 for all the DISPEL derivative models. More implementation details of DISPEL can be found in Appendix D.

4.2. Generalization Efficacy Analysis (RQ1)

To evaluate the generalization performance of the proposed DISPEL framework, we compare the results with 12 baseline methods on five datasets. We summarize the results comparing DISPEL to other baselines based on a ResNet50 pre-trained model in Tab. 1. Overall, DISPEL achieves state-of-the-art without using domain labels. DISPEL achieves the best average accuracy on unseen test domains in 4 out of 5 benchmark datasets. On average, DISPEL shows the best accuracy on unseen test domains over 5 benchmarks, meaning that it has stable effectiveness across different data distributions. Considering the extensive experimentation conducted on 5 benchmark datasets and 22 unseen test domains, the results conclusively demonstrate the efficacy of DISPEL in improving the diverse types of image data.

Table 2: Average unseen test domain accuracy improvement for ERM (ResNet18).

	PACS	Office-Home	Avg.
Group 1: algorithms requiring domain labels			
Mixup [46]	82.3 ± 0.4	64.3 ± 0.2	73.3
CORAL [35]	82.8 ± 0.1	64.0 ± 0.3	73.4
MMD [25]	83.2 ± 0.2	64.2 ± 0.1	73.7
DANN [17]	83.6 ± 0.8	62.6 ± 0.5	73.1
Group 2: algorithms without requiring domain labels			
ERM [40]	82.1 ± 0.1	63.0 ± 0.1	72.6
DRO [32]	82.2 ± 0.2	63.9 ± 0.2	73.1
RSC [19]	83.6 ± 0.2	63.4 ± 0.3	73.5
DISPEL	85.4 ± 0.1	67.2 ± 0.0	76.3

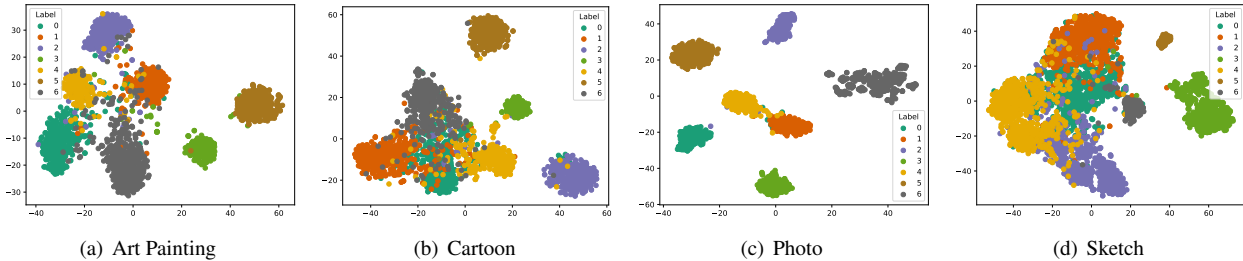


Figure 3: t-SNE visualization of ERM embedding in four unseen test domains of PACS.

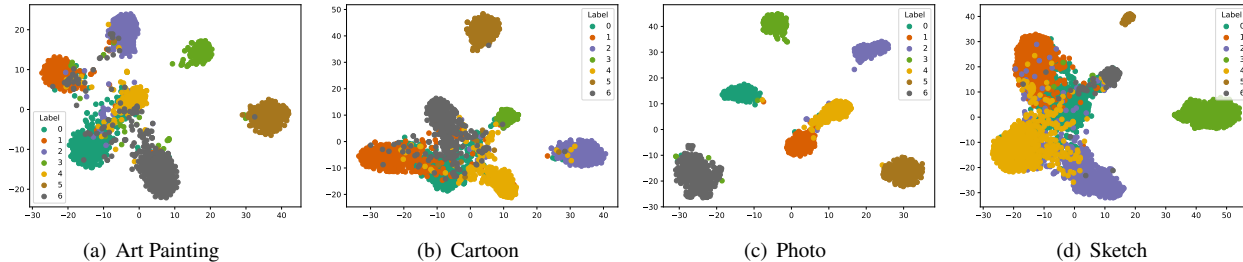


Figure 4: t-SNE visualization of DISPEL embedding in four unseen test domains of PACS.

Table 3: Each unseen test domain accuracy comparisons of PACS (ResNet50).

	Art Painting	Cartoon	Photo	Sketch
Group 1: algorithms requiring domain labels				
Mixup [46]	89.3 \pm 0.5	81.7 \pm 0.1	97.3 \pm 0.4	82.3 \pm 0.8
MLDG [23]	89.1 \pm 0.9	78.8 \pm 0.7	97.0 \pm 0.9	74.4 \pm 2.0
CORAL [35]	84.7 \pm 0.6	81.5 \pm 1.1	96.7 \pm 0.0	81.7 \pm 0.1
MMD [25]	84.5 \pm 0.6	79.7 \pm 0.7	97.5 \pm 0.4	78.1 \pm 1.3
DANN [17]	87.1 \pm 0.5	83.2 \pm 1.4	96.5 \pm 0.2	79.8 \pm 2.8
C-DANN [27]	84.0 \pm 0.9	78.5 \pm 1.5	97.0 \pm 0.4	71.8 \pm 3.9
Group 2: algorithms without requiring domain labels				
ERM [40]	83.7 \pm 0.1	81.8 \pm 1.3	96.7 \pm 0.0	83.4 \pm 0.9
IRM [1]	85.0 \pm 1.6	77.6 \pm 0.9	96.7 \pm 0.3	78.5 \pm 2.6
DRO [32]	85.0 \pm 0.3	81.8 \pm 0.8	96.1 \pm 0.3	84.3 \pm 0.7
RSC [19]	87.8 \pm 0.8	80.3 \pm 1.8	97.7 \pm 0.3	81.5 \pm 1.2
DISPEL	87.1 \pm 0.1	82.5 \pm 0.0	98.0 \pm 0.1	85.2 \pm 0.1

To evaluate the efficacy of DISPEL for improving domain generalization performance based on a less generalization architecture, we also conduct the experiments with a ResNet18. Although it cannot improve ResNet18-based ERM to achieve comparable performance with other ResNet50-based baselines, the results in Tab. 2 show an impressive potential of DISPEL for boosting the generalization ability of small pre-trained architectures. The full experimental results of DISPEL can be found in Appendix E. **Observation 1: DISPEL can be adopted to different neural architectures.** Based on the results shown in Tab. 1 and Tab. 2, DISPEL maintains the generalizing efficacy with different architectures. Even being utilized in a small pre-trained model which is known to have worse generalization ability, DISPEL can improve the prediction accuracy in unseen domains.

Table 4: Each unseen test domain accuracy comparisons of Terra Incognita (ResNet50).

	Location 100	Location 38	Location 43	Location 46
Group 1: algorithms requiring domain labels				
Mixup [46]	60.6 \pm 1.3	41.1 \pm 1.8	58.5 \pm 0.8	35.2 \pm 1.1
MLDG [23]	48.5 \pm 3.3	42.8 \pm 0.4	56.8 \pm 0.9	36.3 \pm 0.5
CORAL [35]	48.6 \pm 0.9	42.2 \pm 3.5	55.9 \pm 0.6	38.7 \pm 0.7
MMD [25]	52.2 \pm 5.8	47.0 \pm 0.6	57.8 \pm 1.3	40.3 \pm 0.5
DANN [17]	49.0 \pm 3.8	46.3 \pm 1.7	57.6 \pm 0.8	40.6 \pm 1.7
C-DANN [27]	49.5 \pm 3.8	44.8 \pm 1.0	57.3 \pm 1.1	38.8 \pm 1.7
Group 2: algorithms without requiring domain labels				
ERM [40]	50.8 \pm 0.2	42.5 \pm 0.2	57.9 \pm 1.3	37.6 \pm 1.3
IRM [1]	44.2 \pm 2.7	41.3 \pm 0.6	54.3 \pm 0.2	36.0 \pm 1.7
DRO [32]	31.8 \pm 0.3	43.7 \pm 1.2	58.0 \pm 0.7	36.6 \pm 1.3
RSC [19]	50.2 \pm 2.2	39.2 \pm 1.4	56.3 \pm 1.4	40.8 \pm 0.6
DISPEL	54.7 \pm 0.3	48.1 \pm 0.0	56.3 \pm 0.3	42.3 \pm 0.2

4.3. Manners of Domain-Specific Liberating (RQ2)

As mentioned in Sec. 3, DISPEL aims to enhance the generalizability of fine-tuned models in a fine-grained instance-specific manner, which considers the unique characteristic of each instance to mask embedding. Hence, in addition to the encouraging experimental outcomes demonstrating the generalizing efficacy of the proposed DISPEL, we seek to delve into the detailed mechanisms underlying DISPEL’s performance.

4.3.1 OOD Performance in Each Unseen Test Domain.

To closely investigate the manner of DISPEL, we first observe the prediction accuracy in each unseen test domain. DISPEL can improve the accuracy of the base algorithm

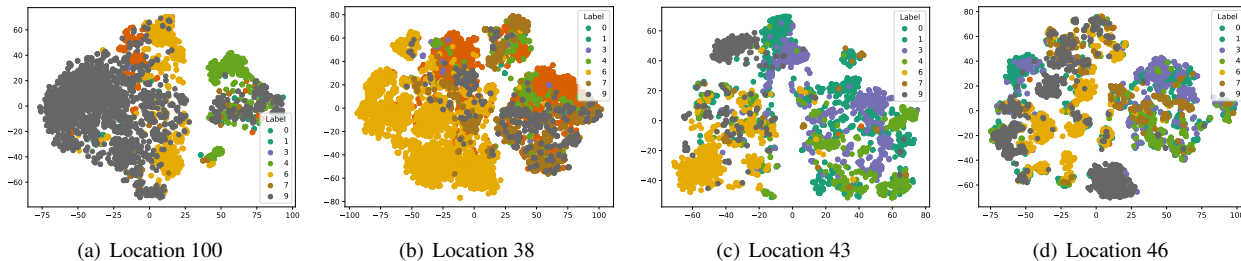


Figure 5: t-SNE visualization of ERM embedding in four unseen test domains of Terra Incognita.

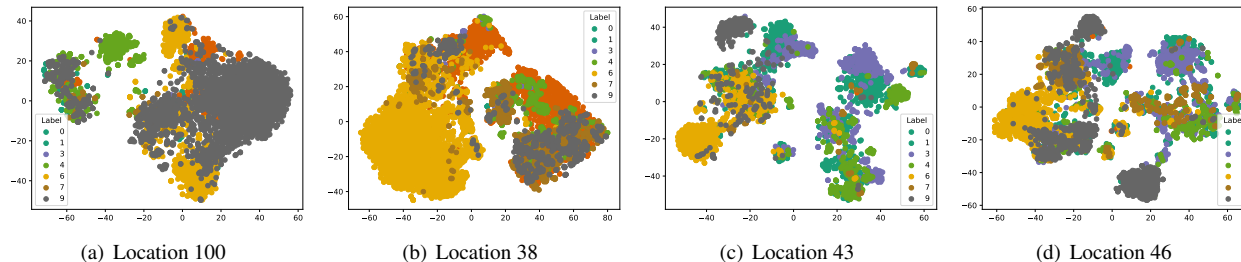


Figure 6: t-SNE visualization of DISPEL embedding in four unseen test domains of Terra Incognita.

(here we use ERM) on 21 out of 22 unseen test domains, except the domain Location 43 of the Terra Incognita dataset.

Tab. 3 shows the accuracy of each unseen test domain of PACS. Despite only achieving the best performance in two unseen test domains, DISPEL can increase the accuracy in all four domains compared to the base algorithm ERM. This phenomenon reflects the instance-specific manner of DISPEL due to the ability of masking data representations according to each input image, which is a more fine-grained perspective than identifying different domain groups for generalization.

Regarding the Terra Incognita, the results show that DISPEL did not enhance accuracy of ERM in the *Location 43* domain, the only one out of 22 domains tested. However, it still has the best performance on average of the four unseen test domains of Terra Incognita. This result again mirrors that the fine-grained instance-specific embedding masking of DISPEL brings a more stable generalizing efficacy among different out-of-distribution sets. Considering the DoainNet as a larger-scale benchmark with a more difficult multi-classification task, DISPEL achieves the best accuracy in five out of six unseen test domains and improve the accuracy in all the unseen domains compared to ERM, as shown in Tab. 5.

Observation 2: DISPEL possesses stable generalizing efficacy. The results show that DISPEL maintains its stable efficacy in improving generalization ability over more different data distributions in more diverse classes of data. And these results reflect the purpose of the EMG module that considers each instance for fine-grained domain-specific feature masking.

Table 5: Each unseen test domain accuracy comparisons of DomainNet (ResNet50).

	Clipart	Infograph	Painting	Quickdraw	Real	Sketch
Group 1: algorithms requiring domain labels						
Mixup [46]	55.3 ± 0.3	18.2 ± 0.3	45.0 ± 1.0	12.5 ± 0.3	57.1 ± 1.2	49.2 ± 0.3
MLDG [23]	59.5 ± 0.0	19.8 ± 0.4	48.3 ± 0.5	13.0 ± 0.4	59.5 ± 1.0	50.4 ± 0.7
CORAL [35]	58.7 ± 0.2	20.9 ± 0.3	47.3 ± 0.3	13.6 ± 0.3	60.2 ± 0.3	50.2 ± 0.6
MMD [25]	54.6 ± 1.7	19.3 ± 0.3	44.9 ± 1.1	11.4 ± 0.5	59.5 ± 0.2	47.0 ± 1.6
DANN [17]	53.8 ± 0.7	17.8 ± 0.3	43.5 ± 0.3	11.9 ± 0.5	56.4 ± 0.3	46.7 ± 0.5
C-DANN [27]	53.4 ± 0.4	18.3 ± 0.7	44.8 ± 0.3	12.9 ± 0.2	57.5 ± 0.4	46.7 ± 0.2
Group 2: algorithms without requiring domain labels						
ERM [40]	58.4 ± 0.3	19.2 ± 0.4	46.3 ± 0.5	12.8 ± 0.0	60.6 ± 0.5	49.7 ± 0.8
IRM [1]	51.0 ± 3.3	16.8 ± 1.0	38.8 ± 2.1	11.8 ± 0.5	51.5 ± 3.6	44.2 ± 3.1
DRO [32]	47.8 ± 0.6	17.1 ± 0.6	36.6 ± 0.7	8.8 ± 0.4	51.5 ± 0.6	40.7 ± 0.3
RSC [19]	55.0 ± 1.2	18.3 ± 0.5	44.4 ± 0.6	12.2 ± 0.6	55.7 ± 0.7	47.8 ± 0.9
DISPEL	63.4 ± 0.1	20.1 ± 0.0	48.2 ± 0.0	14.2 ± 0.0	63.4 ± 0.0	54.9 ± 0.0

4.3.2 Visualization Analysis via t-SNE

To illustrate how DISPEL improves generalization by blocking domain-specific features in the embedding space, we use t-SNE in Fig. 3 to 6 in the unseen test domains of PACS and Terra Incognita by comparing the embedding with and without DISPEL.

Comparing Fig. 3-(a) and Fig. 4-(a), the key observation is that DISPEL aims to make each class more concentrated and separate them better. By drawing down more precise decision boundaries, the predictor can achieve better accuracy in the unseen *Art Painting* domain, in which DISPEL enhances the most accuracy among the 4 domains as shown in Tab. 3. Even when the boundaries between classes are blurred and hard to be separated, DISPEL keeps its impact by making them more concentrated inside each class. For instance, the results on *Sketch* domain, as shown in Fig. 3-(d) and Fig. 4-(d), show that DISPEL concentrates

Table 6: Average unseen test domain accuracy of DISPEL by using other domain generalization algorithms as baselines. It indicates that DISPEL can boost generalization of other algorithms.

	PACS	Office-Home	Avg.
ERM [40]	86.4 \pm 0.1	69.9 \pm 0.1	78.2
ERM w/ DISPEL	88.2 \pm 0.1	73.3 \pm 0.3	80.8
DRO [32]	86.8 \pm 0.4	70.2 \pm 0.3	78.5
DRO w/ DISPEL	88.2 \pm 0.1	72.2 \pm 0.1	80.2
CORAL [35]	86.2 \pm 0.2	70.1 \pm 0.4	78.2
CORAL w/ DISPEL	87.5 \pm 0.1	72.8 \pm 0.2	80.2
DANN [17]	86.7 \pm 1.1	69.5 \pm 0.6	78.1
DANN w/ DISPEL	87.2 \pm 0.0	72.9 \pm 0.3	80.1
Mixup [46]	87.7 \pm 0.5	71.2 \pm 0.1	79.5
Mixup w/ DISPEL	89.1 \pm 0.1	73.4 \pm 0.1	81.3

the representation of each class, decreasing the length of the boundaries between class 0 and 1, 2, and 4. By decreasing the length of boundaries between different groups, the vague part for classification will be less than the original distribution, which means that the correctness of the predictions in the unseen test domains will increase.

Investigating the embedding of Terra Incognita, a more difficult multi-class classification task dataset, we observe the coherent behavior of DISPEL to its manner in PACS. As shown in Fig. 5-(a)(b)(d) and Fig. 6-(a)(b)(d), DISPEL has the same effect as on *Cartoon* and *Sketch* domain of PACS, which is to reduce the length of decision boundaries between different classes by concentrating distribution of each class. In addition, as shown in Tab. 4, *Location 43* is the only domain in which DISPEL cannot improve its classification accuracy. However, the reason is that we cannot achieve our reproduced ERM the same performance as provided in DomainBed [18], and the accuracy of our reproduced ERM in the *Location 43* domain is 55.1%. Therefore, DISPEL actually improves the accuracy in this unseen test domain by 1.3%. As we can see in Fig. 5-(c) and Fig. 6-(c), each class’s instance embedding is concentrated after employing DISPEL as in other domains.

Observation 3: DISPEL concentrates the distribution of each class embedding. The t-SNE analysis demonstrates the superiority of DISPEL, which improves the domain generalization ability of the fine-tuned ERM by concentrating the distribution of embeddings in the same class. Due to this manner, DISPEL can improve classification accuracy in unseen domains, as shown in Tab. 1 to Tab. 5 and Appendix E.

4.4. Boosting Other Algorithm via DISPEL (RQ3)

In previous experiments, we adopt fine-tuned ERM to be the base model of EMG module in DISPEL. Based on the experimental results showing that the proposed DISPEL framework can improve the prediction performance in unseen domains, we are curious if DISPEL can also enhance

the generalization ability of other algorithms.

To investigate the effectiveness of the proposed DISPEL for other approaches, we conduct experiments by comparing it with different baselines. Specifically, we employ DISPEL for 3 representation learning methods; 1 does not require domain labels (DRO), and the others require domain labels (CORAL and DANN). We also adopt DISPEL for 1 data manipulation method that requires domain labels for training (Mixup). According to Tab. 6, DISPEL can improve the prediction accuracy of all 4 baselines on unseen test domains in the 2 benchmarks. However, the improvements are not consistent across different algorithms. In PACS, the improvement of DANN is insignificant compared with other methods, and the boosts of all four algorithms are less than the increase of ERM. Nevertheless, the improvement of DANN in Office-Home is more significant than all other algorithms. It makes sense when we consider the encoders of each fine-tuned algorithm as a different initial state for training the base model of the EMG component. The reason is that the initial states influence the optimization process and might lead to different model weights.

Furthermore, we observe that the higher initial accuracy of an algorithm does not guarantee better performance after leveraging DISPEL for boosting. In PACS, the fine-tuned Mixup model has the best domain generalization performance compared with the other four fine-tuned models, and DISPEL then boosts it to achieve the highest accuracy in unseen test domains. However, despite the different initial performances of five algorithms in PACS, the accuracy after DISPEL boosting of ERM and DRO achieves the same level when CORAL and DANN cannot reach them. Besides, by leveraging DISPEL in the Office-Home dataset, DANN achieves performance close to ERM and Mixup when DRO performance is slightly lower than other methods.

Observation 4: DISPEL can improve generalization ability for different types of algorithms. The experimental results of utilizing DISPEL in four algorithms demonstrate that DISPEL can improve the generalization performance of fine-tuned models. According to the results shown in Tab. 6, despite Mixup achieving the best performance with DISPEL, ERM can achieve equivalent results via DISPEL without using domain labels during training.

5. Conclusions and Future Work

In this work, we demonstrate the efficacy of masking domain-specific features in embedding space for improving the generalization ability of a fine-tuned prediction model. Based on this observation, we propose a post-processing fine-grained masking framework, DISPEL, by accounting for instance discrepancies to further improve generalization ability. Specifically, DISPEL uses a mask generator that generates a distinct mask for each input data, which is used to filter domain-specific features in embedding space. The

results on five benchmarks demonstrate that DISPEL outperforms the state-of-the-art baselines. Regarding future directions, we plan to explore the potential of exploiting DISPEL for different downstream tasks and various types of input data. To achieve this, we will consider the characteristics of each task and input data, allowing us to design an objective loss that is tailored to their specific requirements.

References

- [1] Martin Arjovsky, Léon Bottou, Ishaan Gulrajani, and David Lopez-Paz. Invariant risk minimization. *arXiv preprint arXiv:1907.02893*, 2019.
- [2] Devansh Arpit, Huan Wang, Yingbo Zhou, and Caiming Xiong. Ensemble of averages: Improving model selection and boosting performance in domain generalization. In Alice H. Oh, Alekh Agarwal, Danielle Belgrave, and Kyunghyun Cho, editors, *Advances in Neural Information Processing Systems*, 2022.
- [3] Andrei Barbu, David Mayo, Julian Alverio, William Luo, Christopher Wang, Dan Gutfreund, Josh Tenenbaum, and Boris Katz. Objectnet: A large-scale bias-controlled dataset for pushing the limits of object recognition models. *Advances in neural information processing systems*, 32, 2019.
- [4] Sara Beery, Grant Van Horn, and Pietro Perona. Recognition in terra incognita. In *Proceedings of the European conference on computer vision (ECCV)*, pages 456–473, 2018.
- [5] Nicolas Carion, Francisco Massa, Gabriel Synnaeve, Nicolas Usunier, Alexander Kirillov, and Sergey Zagoruyko. End-to-end object detection with transformers. In *Computer Vision—ECCV 2020: 16th European Conference, Glasgow, UK, August 23–28, 2020, Proceedings, Part I 16*, pages 213–229. Springer, 2020.
- [6] Junbum Cha, Sanghyuk Chun, Kyungjae Lee, Han-Cheol Cho, Seunghyun Park, Yunsung Lee, and Sungrae Park. Swad: Domain generalization by seeking flat minima. *Advances in Neural Information Processing Systems*, 34:22405–22418, 2021.
- [7] Junbum Cha, Kyungjae Lee, Sungrae Park, and Sanghyuk Chun. Domain generalization by mutual-information regularization with pre-trained models. In *Computer Vision—ECCV 2022: 17th European Conference, Tel Aviv, Israel, October 23–27, 2022, Proceedings, Part XXIII*, pages 440–457. Springer, 2022.
- [8] Chia-Yuan Chang, Cheng-Wei Lu, and Chuan-Ju Wang. A multi-step-ahead markov conditional forward model with cube perturbations for extreme weather forecasting. In *Proceedings of the AAAI Conference on Artificial Intelligence*, volume 35, pages 6948–6955, 2021.
- [9] Prithvijit Chattopadhyay, Yogesh Balaji, and Judy Hoffman. Learning to balance specificity and invariance for in and out of domain generalization. In *Computer Vision—ECCV 2020: 16th European Conference, Glasgow, UK, August 23–28, 2020, Proceedings, Part IX 16*, pages 301–318. Springer, 2020.
- [10] Yue Chen, Yalong Bai, Wei Zhang, and Tao Mei. Destruction and construction learning for fine-grained image recognition. In *Proceedings of the IEEE/CVF conference on computer vision and pattern recognition*, pages 5157–5166, 2019.
- [11] Bowen Cheng, Alex Schwing, and Alexander Kirillov. Per-pixel classification is not all you need for semantic segmentation. *Advances in Neural Information Processing Systems*, 34:17864–17875, 2021.
- [12] Xiyang Dai, Yinpeng Chen, Bin Xiao, Dongdong Chen, Mengchen Liu, Lu Yuan, and Lei Zhang. Dynamic head:

- Unifying object detection heads with attentions. In *Proceedings of the IEEE/CVF conference on computer vision and pattern recognition*, pages 7373–7382, 2021.
- [13] Terrance De Vries, Ishan Misra, Changhan Wang, and Laurens Van der Maaten. Does object recognition work for everyone? In *Proceedings of the IEEE/CVF conference on computer vision and pattern recognition workshops*, pages 52–59, 2019.
- [14] Abhimanyu Dubey, Vignesh Ramanathan, Alex Pentland, and Dhruv Mahajan. Adaptive methods for real-world domain generalization. In *Proceedings of the IEEE/CVF Conference on Computer Vision and Pattern Recognition*, pages 14340–14349, 2021.
- [15] Chen Fang, Ye Xu, and Daniel N Rockmore. Unbiased metric learning: On the utilization of multiple datasets and web images for softening bias. In *Proceedings of the IEEE International Conference on Computer Vision*, pages 1657–1664, 2013.
- [16] Aaron Fisher, Cynthia Rudin, and Francesca Dominici. All models are wrong, but many are useful: Learning a variable’s importance by studying an entire class of prediction models simultaneously. *J. Mach. Learn. Res.*, 20(177):1–81, 2019.
- [17] Yaroslav Ganin, Evgeniya Ustinova, Hana Ajakan, Pascal Germain, Hugo Larochelle, François Laviolette, Mario Marchand, and Victor Lempitsky. Domain-adversarial training of neural networks. *The journal of machine learning research*, 17(1):2096–2030, 2016.
- [18] Ishaan Gulrajani and David Lopez-Paz. In search of lost domain generalization. *arXiv preprint arXiv:2007.01434*, 2020.
- [19] Zeyi Huang, Haohan Wang, Eric P Xing, and Dong Huang. Self-challenging improves cross-domain generalization. In *European Conference on Computer Vision*, pages 124–140. Springer, 2020.
- [20] Pavel Izmailov, Dmitrii Podoprikin, Timur Garipov, Dmitry Vetrov, and Andrew Gordon Wilson. Averaging weights leads to wider optima and better generalization. *arXiv preprint arXiv:1803.05407*, 2018.
- [21] KJ Joseph, Salman Khan, Fahad Shahbaz Khan, and Vineeth N Balasubramanian. Towards open world object detection. In *Proceedings of the IEEE/CVF Conference on Computer Vision and Pattern Recognition*, pages 5830–5840, 2021.
- [22] Aditya Khosla, Tinghui Zhou, Tomasz Malisiewicz, Alexei A Efros, and Antonio Torralba. Undoing the damage of dataset bias. In *Computer Vision—ECCV 2012: 12th European Conference on Computer Vision, Florence, Italy, October 7–13, 2012, Proceedings, Part I 12*, pages 158–171. Springer, 2012.
- [23] Da Li, Yongxin Yang, Yi-Zhe Song, and Timothy Hospedales. Learning to generalize: Meta-learning for domain generalization. In *Proceedings of the AAAI conference on artificial intelligence*, volume 32, 2018.
- [24] Da Li, Yongxin Yang, Yi-Zhe Song, and Timothy M Hospedales. Deeper, broader and artier domain generalization. In *Proceedings of the IEEE international conference on computer vision*, pages 5542–5550, 2017.
- [25] Haoliang Li, Sinno Jialin Pan, Shiqi Wang, and Alex C Kot. Domain generalization with adversarial feature learning. In *Proceedings of the IEEE conference on computer vision and pattern recognition*, pages 5400–5409, 2018.
- [26] Ya Li, Mingming Gong, Xinmei Tian, Tongliang Liu, and Dacheng Tao. Domain generalization via conditional invariant representations. In *Proceedings of the AAAI conference on artificial intelligence*, volume 32, 2018.
- [27] Ya Li, Xinmei Tian, Mingming Gong, Yajing Liu, Tongliang Liu, Kun Zhang, and Dacheng Tao. Deep domain generalization via conditional invariant adversarial networks. In *Proceedings of the European Conference on Computer Vision (ECCV)*, pages 624–639, 2018.
- [28] Xingchao Peng, Qinxun Bai, Xide Xia, Zijun Huang, Kate Saenko, and Bo Wang. Moment matching for multi-source domain adaptation. In *Proceedings of the IEEE/CVF international conference on computer vision*, pages 1406–1415, 2019.
- [29] Xue Bin Peng, Marcin Andrychowicz, Wojciech Zaremba, and Pieter Abbeel. Sim-to-real transfer of robotic control with dynamics randomization. In *2018 IEEE international conference on robotics and automation (ICRA)*, pages 3803–3810. IEEE, 2018.
- [30] Vihari Piratla, Praneeth Netrapalli, and Sunita Sarawagi. Efficient domain generalization via common-specific low-rank decomposition. In *International Conference on Machine Learning*, pages 7728–7738. PMLR, 2020.
- [31] Fengchun Qiao, Long Zhao, and Xi Peng. Learning to learn single domain generalization. In *Proceedings of the IEEE/CVF Conference on Computer Vision and Pattern Recognition*, pages 12556–12565, 2020.
- [32] Shiori Sagawa, Pang Wei Koh, Tatsunori B Hashimoto, and Percy Liang. Distributionally robust neural networks for group shifts: On the importance of regularization for worst-case generalization. *arXiv preprint arXiv:1911.08731*, 2019.
- [33] Yichun Shi, Xiang Yu, Kihyuk Sohn, Manmohan Chandraker, and Anil K Jain. Towards universal representation learning for deep face recognition. In *Proceedings of the IEEE/CVF Conference on Computer Vision and Pattern Recognition*, pages 6817–6826, 2020.
- [34] Robin Strudel, Ricardo Garcia, Ivan Laptev, and Cordelia Schmid. Segmenter: Transformer for semantic segmentation. In *Proceedings of the IEEE/CVF international conference on computer vision*, pages 7262–7272, 2021.
- [35] Baochen Sun and Kate Saenko. Deep coral: Correlation alignment for deep domain adaptation. In *European conference on computer vision*, pages 443–450. Springer, 2016.
- [36] Jingru Tan, Changbao Wang, Buyu Li, Quanquan Li, Wanli Ouyang, Changqing Yin, and Junjie Yan. Equalization loss for long-tailed object recognition. In *Proceedings of the IEEE/CVF conference on computer vision and pattern recognition*, pages 11662–11671, 2020.
- [37] Mingxing Tan, Ruoming Pang, and Quoc V Le. Efficientdet: Scalable and efficient object detection. In *Proceedings of the IEEE/CVF conference on computer vision and pattern recognition*, pages 10781–10790, 2020.
- [38] Josh Tobin, Rachel Fong, Alex Ray, Jonas Schneider, Wojciech Zaremba, and Pieter Abbeel. Domain randomization

- for transferring deep neural networks from simulation to the real world. In *2017 IEEE/RSJ international conference on intelligent robots and systems (IROS)*, pages 23–30. IEEE, 2017.
- [39] Jonathan Tremblay, Aayush Prakash, David Acuna, Mark Brophy, Varun Jampani, Cem Anil, Thang To, Eric Cameracci, Shaad Boochoon, and Stan Birchfield. Training deep networks with synthetic data: Bridging the reality gap by domain randomization. In *Proceedings of the IEEE conference on computer vision and pattern recognition workshops*, pages 969–977, 2018.
- [40] Vladimir N Vapnik. An overview of statistical learning theory. *IEEE transactions on neural networks*, 10(5):988–999, 1999.
- [41] Hemanth Venkateswara, Jose Eusebio, Shayok Chakraborty, and Sethuraman Panchanathan. Deep hashing network for unsupervised domain adaptation. In *Proceedings of the IEEE conference on computer vision and pattern recognition*, pages 5018–5027, 2017.
- [42] Riccardo Volpi and Vittorio Murino. Addressing model vulnerability to distributional shifts over image transformation sets. In *Proceedings of the IEEE/CVF International Conference on Computer Vision*, pages 7980–7989, 2019.
- [43] Riccardo Volpi, Hongseok Namkoong, Ozan Sener, John C Duchi, Vittorio Murino, and Silvio Savarese. Generalizing to unseen domains via adversarial data augmentation. *Advances in neural information processing systems*, 31, 2018.
- [44] Jindong Wang, Cuiling Lan, Chang Liu, Yidong Ouyang, Tao Qin, Wang Lu, Yiqiang Chen, Wenjun Zeng, and Philip Yu. Generalizing to unseen domains: A survey on domain generalization. *IEEE Transactions on Knowledge and Data Engineering*, 2022.
- [45] Wenguan Wang, Tianfei Zhou, Fisher Yu, Jifeng Dai, Ender Konukoglu, and Luc Van Gool. Exploring cross-image pixel contrast for semantic segmentation. In *Proceedings of the IEEE/CVF International Conference on Computer Vision*, pages 7303–7313, 2021.
- [46] Yufei Wang, Haoliang Li, and Alex C Kot. Heterogeneous domain generalization via domain mixup. In *ICASSP 2020-2020 IEEE International Conference on Acoustics, Speech and Signal Processing (ICASSP)*, pages 3622–3626. IEEE, 2020.
- [47] Kun Wei, Muli Yang, Hao Wang, Cheng Deng, and Xianglong Liu. Adversarial fine-grained composition learning for unseen attribute-object recognition. In *Proceedings of the IEEE/CVF International Conference on Computer Vision*, pages 3741–3749, 2019.
- [48] Enze Xie, Jian Ding, Wenhai Wang, Xiaohang Zhan, Hang Xu, Peize Sun, Zhenguo Li, and Ping Luo. Detco: Unsupervised contrastive learning for object detection. In *Proceedings of the IEEE/CVF International Conference on Computer Vision*, pages 8392–8401, 2021.
- [49] Enze Xie, Wenhai Wang, Zhiding Yu, Anima Anandkumar, Jose M Alvarez, and Ping Luo. Segformer: Simple and efficient design for semantic segmentation with transformers. *Advances in Neural Information Processing Systems*, 34:12077–12090, 2021.
- [50] Minghao Xu, Jian Zhang, Bingbing Ni, Teng Li, Chengjie Wang, Qi Tian, and Wenjun Zhang. Adversarial domain adaptation with domain mixup. In *Proceedings of the AAAI Conference on Artificial Intelligence*, volume 34, pages 6502–6509, 2020.
- [51] Shen Yan, Huan Song, Nanxiang Li, Lincan Zou, and Liu Ren. Improve unsupervised domain adaptation with mixup training. *arXiv preprint arXiv:2001.00677*, 2020.
- [52] Hongyi Zhang, Moustapha Cisse, Yann N Dauphin, and David Lopez-Paz. mixup: Beyond empirical risk minimization. *arXiv preprint arXiv:1710.09412*, 2017.
- [53] Sixiao Zheng, Jiachen Lu, Hengshuang Zhao, Xiatian Zhu, Zekun Luo, Yabiao Wang, Yanwei Fu, Jianfeng Feng, Tao Xiang, Philip HS Torr, et al. Rethinking semantic segmentation from a sequence-to-sequence perspective with transformers. In *Proceedings of the IEEE/CVF conference on computer vision and pattern recognition*, pages 6881–6890, 2021.

Appendix

A. Proof of Theorem 1

Theorem 1 (Generalization Error Bound). Let $\tilde{\mathbf{x}}_k^T$ be a masked instance of \mathbf{x}_k^T on an unseen domain \mathcal{T} . Given an instance embedding \mathbf{z}_k^T satisfies the composition of domain-specific \mathbf{z}_k^{T-sh} and domain-sharing \mathbf{z}_k^{T-sp} , where $\hat{f}(\mathbf{x}_k^T) = \hat{c}(\mathbf{z}_k^T)$ be the predicted outcomes. For arbitrary distance function $d(\cdot, \cdot)$ in metric space, the generalization error $\mathbf{GE} = \mathbf{E}_{\mathcal{X}}[d(f(\mathbf{x}_k^T), \hat{f}(\tilde{\mathbf{x}}_k^T))]$ of DISPEL framework can be bounded as:

$$\mathbf{GE} \leq \mathbf{E}_{\mathcal{X}}[d(c(\mathbf{z}_k^{T-sh}), \hat{c}(\tilde{\mathbf{z}}_k^{T-sh}))] + \mathbf{E}_{\mathcal{X}}[d(c(\mathbf{z}_k^{T-sp}), \hat{c}(\tilde{\mathbf{z}}_k^{T-sp}))] \quad (5)$$

where $\tilde{\mathbf{z}}_k^T = \mathbf{z}_k^T \odot m_k^T$ is composed of remained domain-specific embedding $\tilde{\mathbf{z}}_k^{T-sp}$ and preserved domain-sharing embedding $\tilde{\mathbf{z}}_k^{T-sh}$.

Proof. In order to estimate the generalization error of DISPEL on unseen domain \mathcal{T} , we calculate the expected values of distance between $f(\mathbf{x}_k^T)$ and $\hat{f}(\tilde{\mathbf{x}}_k^T)$. Hence, the estimated generalization error of \mathcal{T} can be elaborated as:

$$\begin{aligned} \mathbf{GE} &= \mathbf{E}_{\mathcal{T}}[d(f(\mathbf{x}_k^T), \hat{f}(\tilde{\mathbf{x}}_k^T))] \\ &= \int_{\mathcal{X}} d(f(\mathbf{x}_k^T), \hat{f}(\tilde{\mathbf{x}}_k^T)) P(\mathcal{T}) d\mathcal{T} \end{aligned} \quad (6)$$

where $P(\mathcal{T})$ denotes cumulative distribution function of \mathcal{T} . As a lower generalized error \mathbf{GE} represents better generalization capability, we can observe from Eq. 6 that the closer $d(f(\mathbf{x}_k^T), \hat{f}(\tilde{\mathbf{x}}_k^T))$ approaches zero, the better generalization capability is obtained.

In this manner, we now discuss the upper bound of $d(f(\mathbf{x}_k^T), \hat{f}(\tilde{\mathbf{x}}_k^T))$. This also ensures the upper bound of \mathbf{GE} . Following the properties that each instance's embedding \mathbf{z}_k^T can be composed of domain-specific \mathbf{z}_k^{T-sh} and domain-sharing \mathbf{z}_k^{T-sp} , we consider upper bound as follows,

$$\begin{aligned} d(f(\mathbf{x}_k^T), \hat{f}(\tilde{\mathbf{x}}_k^T)) &= d(c(\mathbf{z}_k^T), \hat{c}(\tilde{\mathbf{z}}_k^T)) \\ &= d(c(\mathbf{z}_k^{T-sh} + \mathbf{z}_k^{T-sp}), \hat{c}(\tilde{\mathbf{z}}_k^{T-sh} + \tilde{\mathbf{z}}_k^{T-sp})) \end{aligned} \quad (7)$$

Since $c(\cdot)$ is the linear predictor, we can now recast the Eq. 7 in the following,

$$\begin{aligned} d(f(\mathbf{x}_k^T), \hat{f}(\tilde{\mathbf{x}}_k^T)) &= d(c(\mathbf{z}_k^{T-sh} + \mathbf{z}_k^{T-sp}), \hat{c}(\tilde{\mathbf{z}}_k^{T-sh} + \tilde{\mathbf{z}}_k^{T-sp})) \\ &= d(c(\mathbf{z}_k^{T-sh}) + c(\mathbf{z}_k^{T-sp}), \hat{c}(\tilde{\mathbf{z}}_k^{T-sh}) + \hat{c}(\tilde{\mathbf{z}}_k^{T-sp})) \\ &\leq d(c(\mathbf{z}_k^{T-sh}), \hat{c}(\tilde{\mathbf{z}}_k^{T-sh})) + d(c(\mathbf{z}_k^{T-sp}), \hat{c}(\tilde{\mathbf{z}}_k^{T-sp})) \end{aligned} \quad (8)$$

Following the conclusion of Eq. 6 and Eq. 8, we have the

upper bound of \mathbf{GE} as follows:

$$\begin{aligned} \mathbf{GE} &= \mathbf{E}_{\mathcal{T}}[d(f(\mathbf{x}_k^T), \hat{f}(\tilde{\mathbf{x}}_k^T))] \\ &= \int_{\mathcal{X}} d(f(\mathbf{x}_k^T), \hat{f}(\tilde{\mathbf{x}}_k^T)) P(\mathcal{T}) d\mathcal{T} \\ &\leq \int_{\mathcal{X}} [d(c(\mathbf{z}_k^{T-sh}), \hat{c}(\tilde{\mathbf{z}}_k^{T-sh})) + d(c(\mathbf{z}_k^{T-sp}), \hat{c}(\tilde{\mathbf{z}}_k^{T-sp}))] P(\mathcal{T}) d\mathcal{T} \\ &= \int_{\mathcal{X}} d(c(\mathbf{z}_k^{T-sh}), \hat{c}(\tilde{\mathbf{z}}_k^{T-sh})) P(\mathcal{T}) d\mathcal{T} + \\ &\quad \int_{\mathcal{X}} d(c(\mathbf{z}_k^{T-sp}), \hat{c}(\tilde{\mathbf{z}}_k^{T-sp})) P(\mathcal{T}) d\mathcal{T} \\ &= \mathbf{E}_{\mathcal{X}}[d(c(\mathbf{z}_k^{T-sh}), \hat{c}(\tilde{\mathbf{z}}_k^{T-sh}))] + \mathbf{E}_{\mathcal{X}}[d(c(\mathbf{z}_k^{T-sp}), \hat{c}(\tilde{\mathbf{z}}_k^{T-sp}))] \end{aligned}$$

□

B. Related Works

There are two primary branches of research in the field of domain generalization: data manipulation and representation learning.

Data Manipulation. The data manipulation branch aims to reduce overfitting by increasing the diversity and quantity of available training data. This is typically achieved through the use of data augmentation methods or generative models [38, 29, 39, 43, 52, 50, 51, 46].

Representation Learning. Representation learning is another branch of methods that focuses on training an encoder that maps samples to a latent space where the embedding remains invariant to various domains [1, 32, 19, 23, 25, 17, 7]. Alternative approaches for achieving invariant learning have been proposed, including techniques such as correlation alignment [35], class-conditional adversarial learning [26], minimizing maximum mean discrepancy [27], and mutual information regularization [7] that doesn't require domain labels.

Ensemble Learning. There are some ensemble approaches for domain generalization, which train multiple models and then combine the predictions of these models at validation time to obtain a most generalization model. For instance, SWAD [6] aims to find a flatter minima and suffers less from overfitting than vanilla SWA [20] by a dense and overfit-aware stochastic weight sampling strategy; EoA [2] finds that an ensemble of moving average models outperforms a traditional ensemble of unaveraged models.

C. Datasets Details

To compare the efficacy of our proposed framework with existing algorithms, we conduct our experiments on 5 real-world benchmark datasets: PACS [24], Office-Home [41], VLCS [15], Terra Incognita [4], and DomainNet [28]. Specifically, PACS includes four image styles (Photo, Art, Cartoon, and Sketch), which are considered 4 different do-

mains, and each domain has 7 classes of images (Dog, Elephant, Giraffe, Horse, Person, Guitar, and House) for training and testing. It contains a total of 9,991 instances in 4 domains. Office-Home consists of 65 classes of images for training and testing. These images belong to four image styles (Art, Clipart, Product, Real) being considered as 4 different domains. It contains a total of 15,588 instances in 4 domains. VLCS includes images collected from 4 different datasets (Caltech101, LabelMe, SUN09, and VOC2007), which are considered 4 different domains, and each domain has 5 classes (Dog, Bird, Person, Car, and Chair) for training and testing. It contains a total of 10,729 instances in 4 domains. Terra Incognita consists of 10 classes of photographs of wild animals taken at 4 different locations (Location 100, Location 38, Location 43, and Location 46), considered as 4 different domains. For our experiments, we use the downloader of DomainBed [18] to download the same version Terra Incognita dataset as theirs. It contains a total of 24,788 instances in 4 domains. DomainNet includes 6 image styles (Clipart, Infograph, Painting, Quickdraw, Real, Sketch) considered as 6 different domains. In each domain, there are 345 classes for training and testing. It contains a total of 586,575 instances in 6 domains. DomainNet can be considered a larger-scale dataset with a more difficult multi-classification task than the other 4 benchmarks.

D. Baselines and Implementation Details

Baselines. To fairly compare our proposed framework with existing algorithms, we follow the settings of DomainBed [18] and DeepDG [44], using the best result between DomainBed, DeepDG, and the original literature. The comparisons include 12 baseline algorithms: ERM [40], IRM [1], DRO [32], RSC [19], Mixup [46], MLDG [23], CORAL [35], MMD [25], DANN [17], C-DANN [27], DA-ERM [14], and MIRO [7]. Considering that domain labels can be leveraged as additional information for learning representations mitigating domain-specific features projected to embedding space, we categorize the 12 baseline algorithms into two groups: **Group 1:** the algorithms requiring domain labels (Mixup, MLDG, CORAL, MMD, DANN, C-DANN, and DA-ERM); and **Group 2:** the algorithms without requiring domain labels (ERM, IRM, DRO, RSC, and MIRO).

Note that in Tab. 2, except the results of ERM and our DISPEL are reproduced based on DeepDG [44], the results of other baselines are provided by the GitHub of the same survey paper.

Implementation. All the experimental results of the proposed DISPEL are implemented and performed based on the codebase of DeepDG [44]. Unlike DomainBed [18], our implementation does not use any data augmentation during training. Regarding the setting of model selection,

Table 7: Hyper-parameters of DISPEL based on ERM.

	PACS	Office-Home	VLCS	TerraInc	DomainNet
DNN Architecture: ResNet-18					
Batch size	128	128	128	128	128
Learning rate	1×10^{-3}	1×10^{-3}	3×10^{-4}	1×10^{-4}	1×10^{-4}
τ	0.1	0.1	0.1	0.1	0.1
DNN Architecture: ResNet-50					
Batch size	64	64	64	64	64
Learning rate	5×10^{-5}	1×10^{-3}	1×10^{-3}	2×10^{-4}	1×10^{-4}
τ	0.1	0.1	0.1	0.1	0.1

we use traditional *training-domain validation set* for our implementation, which does not require utilizing domain labels to split the desired validation set. For all the experimental results of DISPEL, we employ ERM algorithm to fine-tune the ResNet-18 and ResNet-50 as the fine-tuned model mentioned in Sec. 3.1. Concerning the use of the EMG, we utilize ResNet50 as the base model for EMG since the 5 domain generalization benchmarks we tested are image datasets.

DNN Architectures. The experimental results are all fine-tuned on the basis of ResNets. Since larger ResNets are known to have better generalization ability, we mainly conduct experiments with ResNet-50 models for all 5 benchmark datasets, and we also conduct the results of DISPEL based on ResNet-18 as a reference shown in Tab. 2. For both the two base network architectures, we both use the ResNet-18 and ResNet-50 pre-trained on ImageNet. As for the EMG component in DISPEL, we employ a ResNet50 pre-trained on ImageNet as the base model.

Table 8: Hyper-parameters of DISPEL for boosting other algorithms, where the DNN architecture is ResNet-50.

	DRO	CORAL	DANN	Mixup
Dataset: PACS				
Batch size	64	64	64	64
Learning rate	1×10^{-3}	1×10^{-3}	5×10^{-3}	5×10^{-4}
τ	0.1	0.1	0.1	0.1
Dataset: Office-Home				
Batch size	64	64	64	64
Learning rate	1×10^{-3}	1×10^{-3}	1×10^{-3}	1×10^{-3}
τ	0.1	0.1	0.1	0.1

D.1. Hyper-parameters of DISPEL

In the proposed DISPEL framework, the hyper-parameters are composed of batch size, learning rate, and τ in Eq. 1, where τ is the only hyper-parameter that is related to our algorithm. The hyper-parameters of DISPEL for each benchmark dataset are shown in Tab. 7.

Table 9: Each unseen test domain accuracy of DISPEL.

Dataset: PACS						
	Art Painting	Cartoon	Photo	Sketch	-	-
DISPEL (ResNet-18)	83.6 \pm 0.3	79.0 \pm 0.2	97.0 \pm 0.0	81.8 \pm 0.0	-	-
DISPEL (ResNet-50)	87.1 \pm 0.1	82.5 \pm 0.0	98.0 \pm 0.1	85.2 \pm 0.1	-	-
Dataset: Office-Home						
	Art	Clipart	Product	Real	-	-
DISPEL (ResNet-18)	61.4 \pm 0.0	53.9 \pm 0.2	76.0 \pm 0.1	77.8 \pm 0.0	-	-
DISPEL (ResNet-50)	71.3 \pm 0.5	59.4 \pm 0.4	80.3 \pm 0.3	82.1 \pm 0.0	-	-
Dataset: VLCS						
	Caltech101	LabelMe	SUN09	VOC2007	-	-
DISPEL (ResNet-18)	97.2 \pm 0.0	62.6 \pm 0.1	75.0 \pm 0.1	76.9 \pm 0.1	-	-
DISPEL (ResNet-50)	98.3 \pm 0.4	65.3 \pm 0.1	77.2 \pm 0.1	76.3 \pm 0.1	-	-
Dataset: Terra Incognita						
	Location 100	Location 38	Location 43	Location 46	-	-
DISPEL (ResNet-18)	44.4 \pm 0.4	49.6 \pm 0.7	48.1 \pm 0.2	37.3 \pm 0.1	-	-
DISPEL (ResNet-50)	54.7 \pm 0.3	48.1 \pm 0.0	56.3 \pm 0.3	42.3 \pm 0.2	-	-
Dataset: DomainNet						
	Clipart	Infograph	Painting	Quickdraw	Real	Sketch
DISPEL (ResNet-18)	44.6 \pm 0.0	14.2 \pm 0.0	39.7 \pm 0.0	10.3 \pm 0.0	45.6 \pm 0.0	40.8 \pm 0.0
DISPEL (ResNet-50)	63.4 \pm 0.0	20.1 \pm 0.1	48.2 \pm 0.0	14.2 \pm 0.0	63.4 \pm 0.0	54.9 \pm 0.0

D.2. Hyper-parameters of DISPEL for Boosting Other Algorithms

As shown in Sec. 4.4, we leverage our DISPEL to further improve the prediction performance on unseen test domain for four existing domain generalization algorithms on PACS and Office Home, where all the DNN architectures are ResNet-50. The hyper-parameters of the DISPEL derivative models for the two datasets are shown in Tab. 8.

E. Experimental Results of DISPEL

To closely investigate the fine-grained behavior of DISPEL in Sec. 4.3, we observe the prediction accuracy in each unseen test domain of all five domain generalization benchmark datasets. In Tab. 9, we show the experimental results of DISPEL on each unseen domain of five domain generalization benchmark datasets based on the two DNN architectures, ResNet-18 and ResNet-50. Based on the experimental results on each unseen domain, we conclude the **Observation 2: DISPEL possesses stable generalizing efficacy.** The results show that DISPEL maintains its stable efficacy in improving generalization ability over more different data distributions in more diverse classes of data. And these results reflect the purpose of the EMG module that considers each instance for fine-grained domain-specific feature masking.

F. Visualization Analysis via t-SNE

To illustrate how DISPEL improves generalization by blocking domain-specific features in the embedding space, we use t-SNE in the unseen test domains of all five benchmark datasets by comparing the embedding with and without DISPEL, as shown in Fig. 7 to Fig. 16. The key observation is that DISPEL aims to make each class more concentrated and separate them better. Taking PACS as an example, by drawing down more precise decision boundaries, the predictor can achieve better accuracy in the unseen *Art Painting* domain, in which DISPEL enhances the most accuracy among the 4 domains as shown in Tab. 3. Even in *Cartoon* domain where DISPEL only raises 0.7% accuracy, it shows the same intention to concentrate the embedding distribution for each class in Fig. 7-(b) and Fig. 8-(b). As for the unseen *Photo* domain, the base algorithm ERM has performed 96.7% accuracy, which means that Fig. 7-(c) reveals what a high-quality representation looks like. Compared to Fig. 8-(c), DISPEL follows the initial distribution and ameliorates the embedding to compress the distributions of each class.

Based on the t-SNE visualization analysis, we conclude **Observation 3: DISPEL concentrate the distribution of each class embedding.** The t-SNE analysis demonstrates the superiority of DISPEL, which improves the domain generalization ability of the fine-tuned ERM by concentrating the distribution of embeddings in the same class.

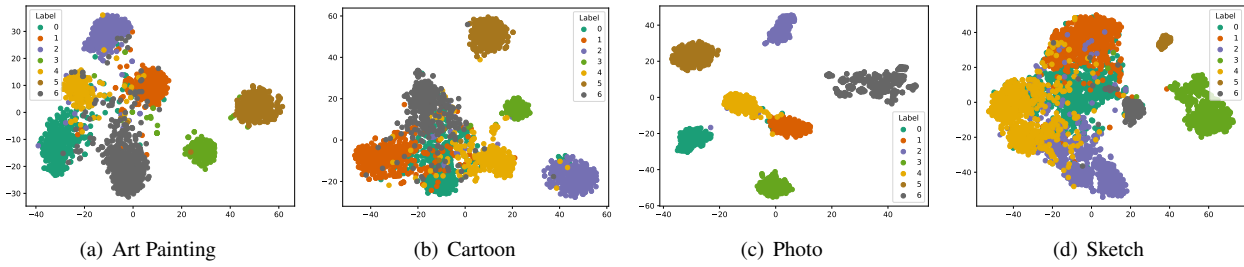


Figure 7: t-SNE visualization of ERM embedding in four unseen test domains of PACS.

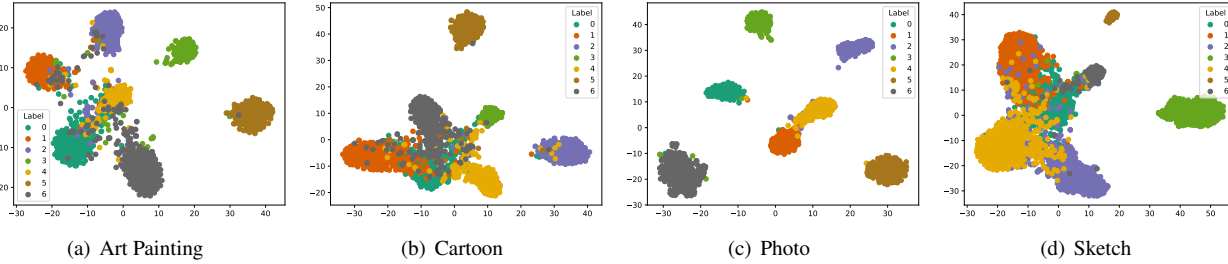


Figure 8: t-SNE visualization of DISPEL embedding in four unseen test domains of PACS.

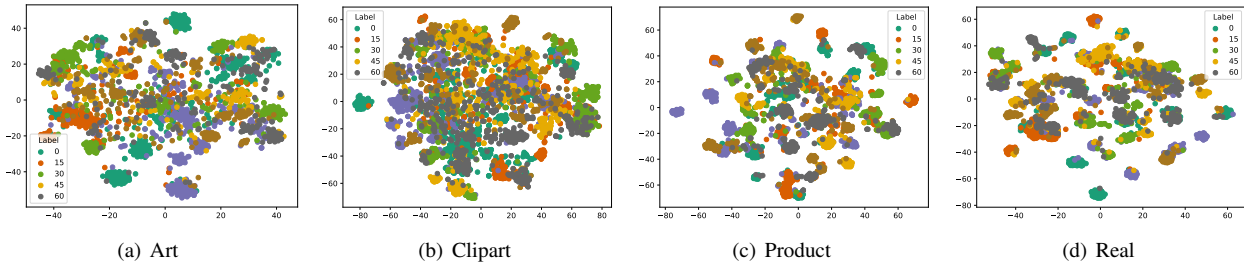


Figure 9: t-SNE visualization of ERM embedding in four unseen test domains of Office-Home.

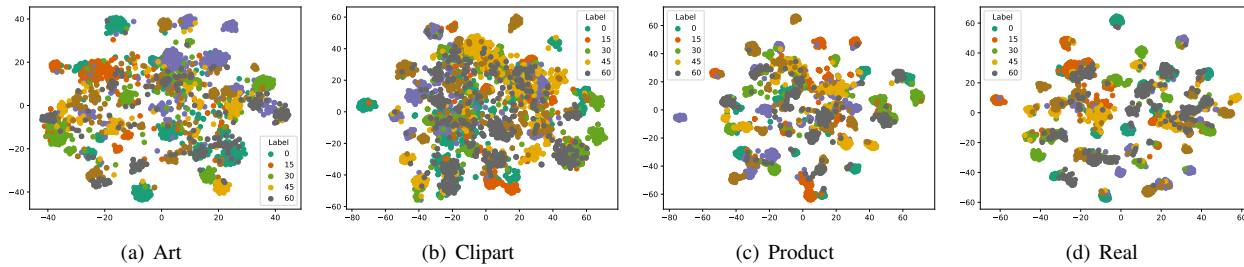


Figure 10: t-SNE visualization of DISPEL embedding in four unseen test domains of Office-Home.

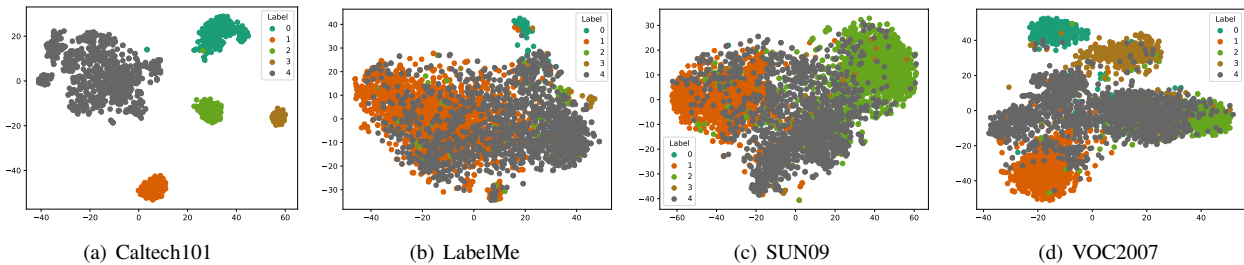


Figure 11: t-SNE visualization of ERM embedding in four unseen test domains of VLCS.

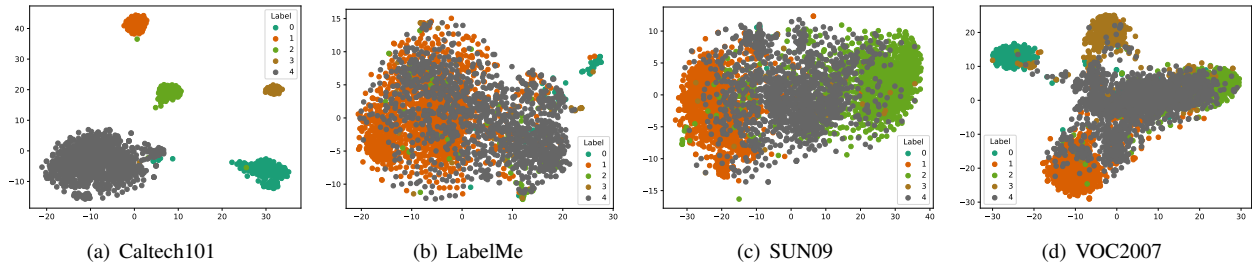


Figure 12: t-SNE visualization of DISPEL embedding in four unseen test domains of VLCS.

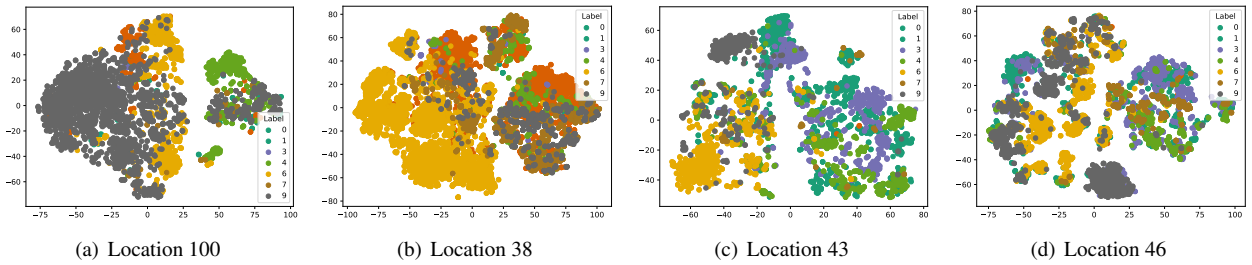


Figure 13: t-SNE visualization of ERM embedding in four unseen test domains of Terra Incognita.

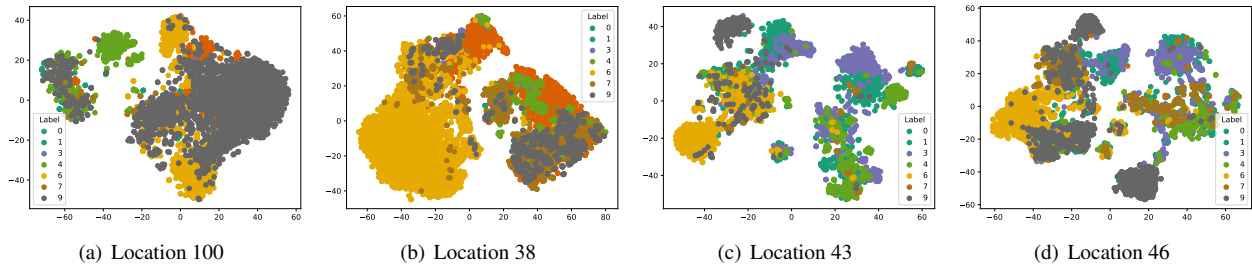


Figure 14: t-SNE visualization of DISPEL embedding in four unseen test domains of Terra Incognita.

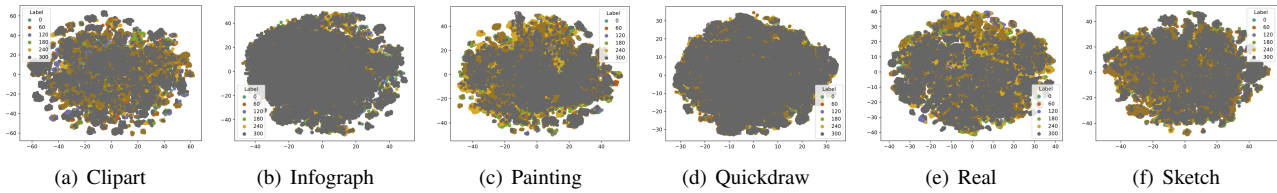


Figure 15: t-SNE visualization of ERM embedding in six unseen test domains of DomainNet.

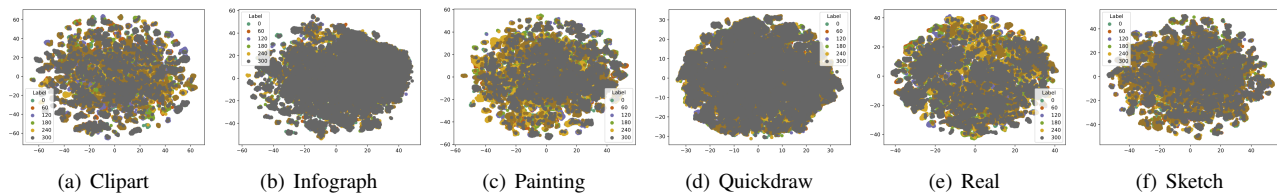


Figure 16: t-SNE visualization of DISPEL embedding in six unseen test domains of DomainNet.